



Published in final edited form as:

Pain. 2018 September ; 159(9): 1856–1866. doi:10.1097/j.pain.0000000000001282.

Chronic neuropathic pain reduces opioid receptor availability with associated anhedonia in rat

Scott J Thompson^{a,c}, Mark H Pitcher^a, Laura S. Stone^c, Farid Tarum^a, Gang Niu^b, Xiaoyuan Chen^b, Dale O. Kiewewetter^b, Petra Schweinhardt^c, and M. Catherine Bushnell^a

^aDivision of Intramural Research, National Center for Complementary and Integrative Health, National Institutes of Health, Bethesda, Maryland; 35A Convent Drive (room 1E-450), Bethesda, Maryland, 20892 USA

^bDivision of Intramural Research, National Institute of Biomedical Imaging and Bioengineering, National Institutes of Health, Bethesda, Maryland; 10 Center Drive (room B2C315), Bethesda, Maryland, 20814 USA

^cFaculty of Dentistry, McGill University, Montreal, QC, Canada; 740 Dr. Penfield Avenue (Suite 3200), Montreal, QC H3A 0G1

Abstract

The opioid system plays a critical role in both the experience and management of pain. While acute activation of the opioid system can lead to pain relief, the effects of chronic pain on the opioid system remain opaque. Cross-sectional positron emission tomography (PET) studies show reduced availability of brain opioid receptors in chronic pain patients, but are unable to (i) determine if these changes are due to the chronic pain itself or to pre-existing or medication-induced differences in the endogenous opioid system, and (ii) identify the neurobiological substrate of reduced opioid receptor availability. We investigated these possibilities using a well-controlled longitudinal study design in rat. Using [¹⁸F]-FDPN-PET in either sham rats (n=17) or spared nerve injury rats (SNI; n=17), we confirmed reduced opioid receptor availability in insula, caudate-putamen and motor cortex of nerve injured rats three-months post-surgery, indicating that painful neuropathy altered the endogenous opioid system. Immunohistochemistry showed reduced expression of the mu-opioid receptor, MOR1, in caudate-putamen and insula. Neither the opioid peptide enkephalin nor the neuronal marker NeuN differed between groups. In nerve-injured animals, sucrose preference, a measure of anhedonia/depression-like behavior, positively correlated with PET opioid receptor availability and MOR1-immunoreactivity in the caudate-putamen. These findings provide new evidence that the altered supraspinal opioid receptor availability observed in human chronic pain patients may be a direct result of chronic pain. Moreover, reduced opioid receptor availability seems to reflect decreased receptor expression, which may contribute to pain-induced depression.

Corresponding author: Mark H. Pitcher, Ph.D., National Center for Complementary and Integrative Health, National Institutes of Health, 35A Convent Drive, RM. 1E420, Bethesda, MD 20892, mark.pitcher@nih.gov.

Conflict of interest: The authors declare no competing financial interests.

1. INTRODUCTION

Opioid analgesics are not equally efficacious for every chronic pain patient [8; 12; 38]. While mechanisms of inter-individual differences in efficacy of opioid analgesics are largely unclear, mounting evidence from positron emission tomography (PET) studies in a variety of chronic pain conditions indicates that, compared to controls, patients have reduced opioid receptor availability in the brain [7; 18; 21; 25–27; 30; 32; 50; 55]. However, cross-sectional studies in patients with variable genetics and exposure to analgesic medications are unable to reveal if altered receptor availability is due to the chronic pain itself or to either a pre-existing or medication-induced difference in the endogenous opioid system. Furthermore, the neurobiological mechanism of reduced availability is equally unclear, where reduced receptor availability may be due to increased release of endogenous opioids occupying the receptors, reduced opioid receptor expression, or reduced numbers of opioid-expressing neurons. Indeed, while acute pain in healthy subjects can increase endogenous opioid levels in the brain [6; 50; 60–62], it is also possible that either the pain or previous pain treatments reduces the number of opioid receptors, as observed in the spinal cord following nerve injury [44; 46; 47; 58]. Alternatively, reduced availability may also result from a smaller number of opioid-expressing neurons. Reductions in grey matter occur in human chronic pain patients [10; 37] and in rats following nerve injury [49]. Diminished opioid receptor expression or neuronal loss both represent a fundamental remodeling in the brain that alters the capacity of those regions to respond to endogenous or exogenous opioids, and could underlie the lack of opioid efficacy in chronic pain. Given the endogenous opioid system's central role in pain, reward and addiction, changes to this system could also impact mental health. Both human chronic pain patients and rodents sometimes exhibit anhedonia (an inability to derive pleasure from normally rewarding stimuli) as well as functional and anatomical changes in the reward system [31; 37; 56]. Thus, it is possible that reduced opioid receptor availability in chronic pain is related to the expression of anhedonia. These questions are best addressed using pre-clinical rodent models, where longitudinal studies controlling genetics, environment, and opioid exposure can be performed. We used a pre-clinical pain model along with tools that allow for direct comparison to the clinical studies. We employed the same clinical *in vivo* brain imaging tool (PET) and opioid tracer ($[^{18}\text{F}]$ -FDPN) in a rat model of intractable neuropathic pain (Spared Nerve Injury; SNI), so that tissue could be extracted and evaluated using immunohistochemistry to investigate the cellular and molecular basis of the observed changes.

2. MATERIALS AND METHODS

2.1. Overview

As summarized in Figure 1, all rats were processed as a single cohort with a minimum period of 48 hours between each procedure. In brief, rats underwent housing acclimation (3 to 4 weeks pre-surgery), baseline sucrose preference (2 to 3 weeks pre-surgery), baseline sensory testing (1 week pre-surgery), pain induction surgery or sham surgery (week 0), post-surgical sensory testing (week 1), three month sensory and behavior testing (weeks 11 to 12), PET brain imaging (weeks 12 to 13) and fixation (week 14). All procedures were approved by the National Institute of Health NINDS/NIDCD Animal Care and Use

Committee. Standard procedures and precautions for working with radioactive materials were followed and procedures were approved by the National Institute of Health Division of Radiation Safety.

2.2. Subjects

Forty six male Sprague-Dawley rats (150-200 grams, Charles River Laboratories) were pair housed (injured with injured and control with control) in temperature controlled (21.7 to 23.3 C) ventilated racks on an inverted light/dark cycle (lights on from 21:00-09:00). *Ad libitum* access to both food (soy-free diet, Harlan Teklad 2020X) and water was provided. Thirty-four rats (SNI = 17, sham = 17) completed all behavioral testing and FDPN-PET brain imaging. Brain tissue was processed for immunohistochemistry from 16 of these rats (SNI = 8, sham = 8). Exclusion and inclusion criteria are listed within each respective section.

2.3. Neuropathic pain model

The spared nerve injury (SNI) model of neuropathic pain is a well characterized model of peripheral neuropathic pain that results in persistent touch and temperature sensitivity on the injured paw [16]. For this study, rats were randomly assigned to either SNI (24 rats) or sham groups (22 rats, control group). For the procedure, rats were anesthetized with isoflurane (5.0% for induction, 2.0% for maintenance, 1 L/min). The surgery involves exposing the left sciatic nerve by blunt dissection of the biceps femoris muscle. The tibial and common peroneal nerves are ligated (2 on each nerve, 2 to 3 mm separation) and each are sectioned between the ligations. The sural nerve is left intact. Sham surgery (control) is identical with the exception that the sciatic nerve is visualized, but not modified.

2.4. Sensory testing

Prior to behavioral testing, rats were habituated to the room for one hour in their home cages followed by a 30-minute habituation to the testing apparatus. Mechanical sensitivity was measured using a Dynamic Plantar Aesthesiometer (Ugo Basile, Varese, Italy) with a 50 gram peak and 10 second ramp. Thirty minutes after, cold sensitivity was assessed with the acetone test [13]. Fifty μ L of acetone was applied to the plantar surface of the hind paw and the duration of the response (shaking or licking of the paw) that occurred within 1 minute was measured with a stopwatch. One nerve injured rat was excluded from sensory testing at the three month post-surgery time point because the plantar surface of the foot was not accessible with the testing apparatus.

2.5. Sucrose preference

Sucrose preference was used as a measure of anhedonia. Procedures similar to Amarin et al. [2] were followed. To familiarize the rats with the procedure, each rat was placed individually into a clean, empty cage for a period of two hours with one bottle of water and one bottle of 1% sucrose water for 5 consecutive days, alternating the side containing sucrose water daily to minimize learning effects. Three days later, food and water were removed from the home cage at 17:00. At 10:00 on the next day, each rat was placed into a clean cage with pre-weighed bottles of 1% sucrose water and water. Following a period of

one hour the amount of liquid consumed was measured. Sucrose preference testing was repeated at three months post-surgery. One sham rat was excluded from analysis as a result of a bottle leak during the baseline testing procedure. The sucrose preference score was calculated as the proportion of sucrose water consumed pre-surgery and 3-months post-surgery: $(\text{sucrose water consumed}/(\text{sucrose water consumed} + \text{water consumed})) \times 100$.

2.6. Radiochemistry

We opted to use 6-O-(2-[^{18}F]fluoroethyl)-6-O-desmethyldiprenorphine ([^{18}F]FDPN) based in part on the relatively long half-life and short positron range associated with the fluorine-18 (^{18}F) radioisotope. [^{18}F]FDPN is a radioactively labeled PET tracer that is an analog of diprenorphine with a half life of 110 minutes. Like diprenorphine, [^{18}F]FDPN is a non-selective opioid receptor antagonist that binds with equal affinity to mu, delta and kappa. The synthesis followed the method of [53] with some modifications. Specifically, [^{18}F]fluoroethyltosylate was made via an automated procedure. The automatic HPLC trace enrichment method for semipreparative HPLC of final product was not used, different HPLC columns and solid phase extraction columns were used. Lastly, the final product was isolated from HPLC eluate using solid phase extraction.

2.7. PET imaging

After one hour of acclimation to the PET facility, rats were placed in an anesthesia induction chamber with 5% sevoflurane. Rats were removed from the chamber while anaesthesia was maintained with 3% sevoflurane administered via nose cone. Depth of anesthesia was confirmed by non-response to toe pinch. Rats were then given a tail-vein injection of the PET tracer [^{18}F]FDPN (0.6 mCi). Anesthetic was immediately removed and the rats were placed in a 30 cm \times 30 cm \times 30 cm ventilated Plexiglas box. At minute 25 post-injection, rats were removed from the Plexiglas box and anesthetized in an induction chamber with 5% sevoflurane followed by placement on the PET scanner bed (InveonTM small-animal PET scanner, Siemens Healthcare, Erlangen, Germany) in a prone position and maintained under 3% sevoflurane anesthesia administered via nose cone. Body temperature was maintained with a heating pad and sterile ophthalmic ointment was applied to the eyes to prevent desiccation under anaesthesia. PET scanning started at minute 30 post-injection for a period of 30 minutes. Rats with incomplete behavioral data and their cage-mates were excluded from PET imaging. In addition, one production of [^{18}F]FDPN did not result in supraspinal binding and there were two scan acquisition failures. In total, PET data for 17 SNI-operated rats and 17 sham-operated rats were collected and analyzed.

2.8. PET image processing and analysis

Image reconstruction was performed using Siemens microPET Manager Software. An OSEM3D (3 iterations) MAP (18 iterations) algorithm was used to create a single timeframe for the 30 minutes of data in a 128 \times 128 \times 159 matrix with a voxel size of 0.78 \times 0.78 \times 0.80 mm. The files were then converted from the proprietary manufacturer's image file format to the NIFTI file format using (X)MedCon (<http://xmedcon.sourceforge.net/>). To facilitate automated alignment, a block of 30 \times 25 \times 50 voxels centered on the thalamus and containing the whole brain was extracted from each scan.

Registration was performed using a combination of SPM8 (<http://www.fil.ion.ucl.ac.uk/spm/software/spm8/>) and minc tools (<http://www.bic.mni.mcgill.ca/ServicesSoftware/MINC>). The PET scans were aligned to a common space with SPM8 using the PET toolbox with a 1.6 mm smoothing kernel and linear registration algorithm. The group average of the PET scans was then converted to the minc file format to manually coregister a size-matched anatomical rat MRI to the PET space using the software 'register.'

Brain regions relevant to pain and reward were defined on the anatomical rat MRI in Paxinos space [40] to confirm that the tracer was binding as expected in the control rats. Regions of Interest (ROI) defined were the thalamus, anterior insula (Ant Ins), posterior insula (Post Ins), the prelimbic and infralimbic cortex (homologous to the human prefrontal cortex (PFC)), anterior Cg1 and Cg2 (homologous to the human anterior cingulate cortex (ACC)), nucleus accumbens (NAc), caudate putamen (CPu), posterior Cg1 and Cg2 (homologous to human mid cingulate cortex (MCC)), amygdala, secondary somatosensory cortex (S2), visual cortex (V1/V2), periaqueductal grey (PAG), cerebellum and the primary somatosensory cortex (S1). All regions have the right and left hemisphere defined separately with the exception of the cerebellum and a few brain regions located on the midline including PFC, PAG, ACC and MCC. Each PET scan was then normalized using the reference tissue ratio method with a cerebellum mask (eroded to minimize partial volume effects) used as the reference region. The ROI map was applied to each individual sham rat PET image to extract the mean, cerebellum normalized tracer binding within each region.

Group differences between SNI and sham operated rats were evaluated using SPM8 investigating the contrast SNI < sham under the assumption that results would mimic the decrease in opioid receptor availability seen in the clinical PET chronic pain studies. This assumption was verified by checking the SNI > sham contrast. The resultant contrast maps were masked for $z > 2.3$ and cluster-corrected using the SPM8 toolbox VBM8 to calculate the cluster size threshold for a resultant one-tailed, cluster corrected threshold of $p < 0.01$.

2.9. Perfusion fixation

From the 34 rats (SNI = 17, sham = 17) that underwent FDPN-PET brain imaging, 16 (SNI = 8, sham = 8) were selected by randomly choosing one rat from each cage followed by verification that there was no weight difference between the groups. Tissue fixation via intracardial perfusion was based upon the procedures described by Arvidsson et al. [4] using a gravity fed system. In brief, animals were deeply anesthetized with isoflurane, the chest cavity was opened, heart was exposed and a 15-gauge olive-tipped perfusion needle was inserted through the cut ventricle into the ascending aorta and a relief incision was made to the rat's right atrium. Perfusion consisted of 250 ml of vascular rinse (1 L = 50 ml of 0.2 M phosphate buffer solution (PBS) at pH=7.4, 9g NaCl, 0.25g KCl, 0.5g NaHCO₃ and 950 ml distilled water) followed by 1000 ml of fixative (40 g paraformaldehyde diluted in 250 ml distilled water, 400 ml 0.4M PBS, 140 ml saturated picric acid and 210 ml distilled water at pH 6.9) and 500 ml of cryo-protection solution (10% sucrose in 0.2M PBS). Rat brains were extracted and incubated in cryo-protection solution at 4°C for 5 days post-fixation, embedded in OCT cutting medium (Tissue-Tek) and stored at -20°C.

2.10. Immunohistochemistry

From each rat, a total of six sections from each of the two coronal levels of interest were triple labeled to identify the mu-opioid receptor, enkephalin and neurons. Within those two coronal levels, three brain regions were selected for further analysis based upon FDPN-PET results (see results section: ipsilateral caudate-putamen, ipsilateral anterior insula and contralateral posterior insula). Tissue was sectioned on a cryostat at a thickness of 14 μm with 126 μm spacing between each sample to span approximately 1 PET voxel width. The rabbit-derived MOR1 antisera was prepared against a synthetic peptide corresponding to MOP₃₈₄₋₃₉₈ (QLENLEAETAPLP) of the rat MOR1 gene and has been previously determined to be specific for MOR1 based on pre-adsorption studies, Western blot and epitope-expressing cell lines [4]. The MOR1 antibody used here (RRID: AB_2314812; provided by Dr Lucy Vulchanova at the University of Minnesota) was harvested from the same rabbit used by Arvidsson and is well characterized in the opioid receptor research community [4]. The mouse-derived anti-ENK antibody (MAB350; RRID: AB_2268028) and the guinea pig-derived anti-NeuN antibody (ABN90; RRID: AB_11205592) were acquired from EMD Millipore. Sections were washed in 0.01 M PBS then incubated in PBS containing blocking serum (1% normal donkey serum (Jackson ImmunoResearch Labs, West Grove, PA), 1% normal goat serum (Vector Lab, Burlingame, CA) + 1% BSA (Jackson ImmunoResearch Labs, West Grove, PA) and 0.3% Triton X-100) and the three antibodies (NeuN 1:1,000; ENK 1:400; MOR1 1:200) for 18 hours at 4°C. This was followed by incubation in PBS containing 3 separate secondary antibodies conjugated with Alexa Fluor® 488, Alexa Fluor® 594, and Alexa Fluor® 350 (Invitrogen). All steps were carried out at room temperature except where indicated. Washes before and after each step were performed with 0.01 M PBS, 3 times, 3 min each. Finally, all sections were cover-slipped by using Vectashield® without DAPI (Vector Labs).

2.11. Microscopy

Images were collected on an Olympus BX51 fluorescent microscope (Olympus Corporation, Tokyo, Japan). The filter cubes used for each respective fluorophore were Texas Red for Alexa Fluor® 594, DAPI for Alexa Fluor® 350 and FITC for Alexa Fluor® 488. Images were acquired with a UPlanFL N, 20 \times /0.50, ∞ /0.17/FN26.5 on an Olympus DP71 digital camera. Software used to record the images was the Olympus DP Controller 3.2.1.276 at an image size of 4080 \times 3072, iso sensitivity at 200 and saved as uncompressed TIFF. Acquisition time was kept constant across all rats for each section and label with exposure times established by testing sections of non-interest prior to data collection. Location of the regions of interest were selected based upon where the FDPN-PET results were observed (CPu, Bregma 1.68, vertical 3.8, lateral -3.4; Anterior Insula, Bregma 1.68, vertical 3.8, lateral -4.5; Posterior Insula, Bregma -0.72, vertical 3.2, lateral 6.3, stereotaxic coordinates, vertical orientation ventral to dorsal, lateral orientation with left negative and right positive [40]).

2.12. Image analysis

Mu-opioid receptor expression was assessed using immunofluorescence intensity of the MOR1 antibody, similar to the methodology used by [59]. Briefly, images were quantified

using ImageJ v1.50, 64 bit. First, all images were converted to uncompressed greyscale TIFF images with immunofluorescence intensity levels represented by arbitrary units that fall within the range of the bit depth range of the digital camera. MOR1-immunoreactivity (-ir) and ENK-ir were quantified for mean intensity within the full image frame for all regions except the caudate-putamen, where the border between the caudate-putamen and anterior insula is within the image frame. Consequently, for the caudate-putamen, the mean intensity was assessed in the upper-right quadrant of the image (25% of the image, upper-right corner). NeuN cell bodies were counted by making the image binary, performing a watershed split and then performing a particle count with lower limit to the size of the particles set to 500 pixels to eliminate speckle noise from the output. As with MOR-ir and ENK-ir quantification, the NeuN-ir count was performed in the upper-right quadrant of the caudate-putamen images.

2.13. Experimental design and statistical analysis

Sensory and sucrose preference testing—Sample size was determined based upon previous experience, with $n = 45$ (SNI = 23, sham = 22) for sensory testing and $n=45$ (SNI = 24, sham = 21) for sucrose preference (exclusions listed in Methods section). The data were evaluated for outliers ($3\times$ interquartile range), normality (Shapiro-Wilk test, $p < 0.05$) and equal variance (Levene $p < 0.05$). A repeated measures two-way ANOVA was used to assess the data that occurred over multiple time points (two time points for sucrose preference, three time points for all others), with time as a within-subjects factor and surgical group as a between-subjects factor. Post hoc tests using the Bonferroni correction were used to investigate between-subject differences. Given there is no non-parametric equivalent to a repeated measures two-way ANOVA, if the data did not meet the basic assumptions for parametric testing, the analysis was followed up with non-parametric Mann-Whitney U tests at each time point as an additional assessment of the data. Data were processed using SPSS (IBM SPSS, version 20.0.0) and results are reported as mean \pm standard error. Please refer to Section ‘Methods: Sensory testing; Sucrose preference’ for complete details.

PET imaging and analysis—Sample size was determined based upon previous experience, with $n = 34$ (SNI = 17, sham = 17, exclusions listed in Methods section). Multiple comparisons for SNI vs sham contrast were controlled for by using cluster correction. Multiple comparisons for the sham ROI analysis ($n = 17$) were controlled for by using an ANOVA followed with post hoc Bonferroni correction. Data for the sham ROI analysis were processed using SPSS (IBM SPSS, version 20.0.0), and results are reported as mean \pm standard deviation. Please refer to Section ‘Methods: PET image processing and analysis’ for complete details.

Microscopy image analysis—Sample size was determined based upon previous experience with $n = 16$ (SNI = 8, sham = 8, inclusion criteria listed in Methods section). A two-way ANOVA was used to assess the effect of surgical group over the three brain regions for each of the quantified measures (anti-MOR1-ir, anti-ENK-ir and NeuN cell count). Post hoc tests using the Bonferroni correction were used to investigate between subject differences for each brain region. Data were processed using SPSS (IBM SPSS, version

20.0.0) and results are reported as mean \pm standard error. Please refer to Section ‘Methods: Microscopy; Image analysis’ for complete details.

Brain and sucrose preference correlations—Correlations between opioid receptor related measures within caudate-putamen and sucrose preference were assessed with a two-tailed bivariate Pearson’s correlation analysis. Data were processed using SPSS (IBM SPSS, version 20.0.0).

3. RESULTS

3.1. Mechanical and cold hypersensitivity developed with nerve injury

Nerve-injured rats showed profound hypersensitivity to touch and cold one week after surgery that persisted at the three month post-surgery time point (Figure 2A&B). A significant group \times time interaction was observed for mechanical threshold ($F_{2,86} = 94.7$, $p < 0.001$, Figure 2A). Posthoc tests showed no significant pre-surgery mechanical threshold difference between the two groups with pre-operation nerve-injured rats at 33.11 ± 1.32 grams and pre-operation control rats at 33.95 ± 1.70 grams ($p = 0.698$). One week post-operation nerve-injured rats had a significantly lower withdrawal threshold at 1.63 ± 0.14 grams compared to controls at 30.09 ± 1.26 grams ($p < 0.001$). This difference persisted at the three month time point with nerve-injured rats withdrawal threshold at 3.12 ± 0.36 grams and controls at 36.92 ± 1.47 grams ($p < 0.001$). Similarly, cold sensitivity showed a significant group \times time interaction effect ($F_{2,86} = 17.5$, $p < 0.001$, Figure 2B). There was no pre-surgery cold sensitivity difference (SNI = 0.00 ± 0.00 s, sham = 0.02 ± 0.02 s, $p = 0.154$). After surgery, a group difference was observed one week post-surgery (SNI = 2.06 ± 0.31 s, sham = 0.00 ± 0.00 s, $p < 0.001$) which persisted at the three month time point (SNI = 1.69 ± 0.32 s, sham = 0.00 ± 0.00 s, $p < 0.001$).

Due to an outlier and violation of normality and equal variance identified in the sensory data (outlier violation for three month cold sensitivity in nerve-injured rats; normality violations for three month mechanical sensitivity in nerve-injured rats, pre-surgery cold sensitivity in control rats, three month cold sensitivity in nerve-injured rats; homogeneity of variance violations for cold and mechanical sensitivity for all time points except the one week mechanical sensitivity), the mixed ANOVAs were followed up by non-parametric Mann-Whitney U tests at each time point. The outcomes did not change for any of the data assessed. Group differences for mechanical thresholds pre-surgery, one week post-surgery and three months post surgery had p-values of 0.812, < 0.001 and $p < 0.001$, respectively. P-values for cold sensitivity pre-surgery, one week post-surgery and three months post surgery were 0.144, 0.001 and 0.001.

3.2. Sucrose preference decreased with nerve injury

Nerve-injured rats had lower sucrose preference than control animals three months post-surgery, with no group differences in sucrose preference pre-surgery (Figure 2C).

A repeated measures two-way ANOVA revealed a significant group \times time interaction ($F_{1,43} = 5.02$, $p = 0.030$; pre-surgery SNI = $59.92 \pm 3.04\%$, sham = $58.78 \pm 2.35\%$; 3-month SNI = $58.88 \pm 3.56\%$, sham = $68.38 \pm 3.24\%$). Posthoc assessment looking at cross-sectional time

points (which does not take into account the interindividual differences in sucrose preference) found nerve-injured rats had a trend towards less sucrose preference than controls at the three month time point ($p=0.057$) and no difference pre-surgery ($p=0.800$). Due to potential divergence from normality (three month percent sucrose consumed, $p=0.011$), the non-parametric Mann-Whitney U test was used to compare nerve-injured to control rats pre-surgery, three months post-surgery and the difference scores (post-surgery minus pre-surgery sucrose preference for each individual rat to account for interindividual differences in sucrose preference). The non-parametric evaluation also suggests a significant group effect with time with pre-surgery $p = 0.856$, post-surgery $p = 0.053$ and the difference score $p = 0.014$.

3.3. Tracer distribution in controls

In order to validate the tracer methods, we examined binding levels in pain- and reward-related brain regions, many of which have high levels of opioid binding in humans [5; 23]. In the control rats, we found specific binding of [^{18}F]FDPN in all examined regions as shown in Figure 3. A one way ANOVA contrasting all examined brain regions showed an overall difference among sites ($F_{22,368} = 284.251$, $p < 0.001$). Posthoc analysis contrasting each brain region to the cerebellum (reference site) found each region to have significantly greater binding than the cerebellum, which is virtually devoid of opioid receptors [42] ($p < 0.001$). For the brain regions with right and left hemispheric data, an assessment of potential hemispheric differences using a two way ANOVA with brain region and hemisphere as factors showed no significant main effect for hemispheric side ($F_{1,288} = 1.799$, $p = 0.181$).

3.4. Opioid receptor availability decreased with nerve injury

Multiple brain regions showed less opioid receptor availability in the nerve-injured group (Figure 4), whereas no brain region showed more opioid receptor availability (i.e. increased tracer binding) in the nerve-injured group. The cluster threshold was calculated to be 14.341 voxels per cluster. Thresholding clusters to a minimum of 15 voxels, three clusters covering four brain regions were found to have significantly less FDPN tracer binding: ipsilateral anterior insula and ipsilateral caudate-putamen (left side of the brain); contralateral posterior insula; contralateral M1/M2. There were no clusters that exceeded the threshold for statistical inference for the contrast of SNI > sham, nor any single voxels with a voxel-based z-value greater 2.3.

3.5. Immunohistochemistry

We extracted tissue from nerve-injured and control rats from regions showing pain-related reduced receptor availability that overlapped with the human literature (Ant CPu, Ant Insula, Post Insula), and using immunohistochemistry, tissue was labeled for neuronal cell bodies (NeuN), enkephalin (ENK), and mu-opioid receptors (MOR1) as shown in Figure 5.

Neuron count unchanged by nerve injury—The NeuN-ir cell count across the three brain regions was not significantly different between nerve-injured and control rats (Figure 5A, $F_{1,42} = 0.936$, $p = 0.339$). Despite the negative result of the ANOVA, we performed posthoc tests for the individual brain region to demonstrate the lack of any trend [CPu (SNI

= 159 ± 4 ; Sham = 155 ± 5 ; $p = 0.882$), anterior insula (SNI = 630 ± 17 ; Sham = 616 ± 15 ; $p = 0.627$) and posterior insula (SNI = 610 ± 40 ; Sham = 580 ± 18 ; $p = 0.306$).

3.6. Enkephalin-immunoreactivity unchanged by nerve injury

No difference in ENK-ir was observed over three brain regions (Figure 5B, $F_{1,42} = 0.166$, $p = 0.685$) and none of the regions demonstrated any trend for a group difference [CPu (SNI = 10464 ± 525 ; Sham = 11097 ± 487 ; $p = 0.271$), anterior insula (SNI = 8896 ± 412 ; Sham = 8884 ± 273 ; $p = 0.983$) and posterior insula (SNI = 9232 ± 357 ; Sham = 9014 ± 286 ; $p = 0.702$)].

3.7. Mu-opioid receptor immunoreactivity decreased with nerve injury

MOR1-ir across three brain regions differed between nerve-injured and control animals (Figure 5C, $F_{1,42} = 8.092$, $p = 0.007$). Post-hoc tests showed lower mu-opioid receptor label intensity in CPu as well as anterior insula in nerve-injured animals [CPu (SNI = 8437 ± 437 ; Sham = 9832 ± 358 ; $p = 0.048$) and anterior insula (SNI = 8862 ± 452 ; Sham = 10390 ± 398 ; $p = 0.031$)]. Posterior insula was not found to be significantly different between groups (SNI = 9531 ± 620 ; Sham = 9986 ± 587 ; $p = 0.510$).

3.8. Sucrose preference was correlated to opioid receptor availability and MOR-ir

The proportion of sucrose water consumed at the three month time point for all rats was positively correlated with opioid receptor availability in the caudate-putamen cluster ($R=0.353$, $p = 0.041$). As a secondary check, the relationship between the anatomically defined caudate-putamen and sucrose preference was investigated and was found to be significant ($R = 0.360$, $p=0.037$). When the surgical groups were analyzed separately, the nerve-injured animals continued to show a positive correlation between sucrose preference and MOR-ir ($R = 0.500$, $p=0.041$; Figure 6A). In contrast, the sham group did not show this correlation ($R = 0.169$, $p=0.515$).

The proportion of sucrose water consumed for all rats was also positively correlated with MOR1-ir in the caudate-putamen ($R = 0.628$, $p=0.009$). When the surgical groups were analyzed separately, the SNI group continued to have a positive correlation for the CPu as shown in Figure 6B ($R = 0.799$, $p=0.017$), however, the sham group did not ($R = -0.182$, $p=0.667$).

4. DISCUSSION

Our results show that following 3-months of hypersensitivity, nerve-injured rats have decreased opioid receptor availability in the insula, caudate-putamen and motor cortex compared to matched sham controls. *Ex vivo* immunohistochemistry revealed decreased MOR1-ir in the anterior insula and caudate-putamen. Finally, sucrose preference, a rodent assay for anhedonia, positively correlated with opioid receptor availability and MOR1-ir in the caudate-putamen of the injured rats.

4.1. Chronic pain drives reductions in opioid receptor availability in striatum and insula

Human cross-sectional studies showing reduced opioid binding in chronic pain patients cannot determine if reduced binding is caused by the pain condition, pain treatments or represents an intrinsic brain difference in people who might be prone to develop chronic pain. To resolve this issue, we randomly assigned rats in this study to either the control or the injury condition, and ensured identical environmental conditions between groups. Opioid receptor availability was reduced in the nerve-injured group compared to controls, clearly indicating that reduced receptor availability is a result of the nerve injury. In this light, reduced opioid receptor availability in patients may also be at least partially a direct consequence of chronic pain, especially in the subset exhibiting comorbid anhedonia.

As mentioned, a number of clinical studies have investigated opioid receptor availability in chronic pain patients [7; 18; 21; 25–27; 32; 55]. Of these, the most relevant comparison to our study is an investigation of peripheral neuropathic pain patients using the PET tracer [¹¹C]diprenorphine [32]. As in the present study, lower opioid receptor availability was found in the striatum and insula. Lower binding was also seen in thalamus, ACC, posterior temporal and orbitofrontal cortices and posterior midbrain. While the differences observed by Maarrawi et al. were more widespread, the striatum and the insula are among the regions with the most consistently reduced opioid receptor availability across chronic pain conditions [7; 18; 21; 25–27; 32; 55]. Thus, the reduced binding observed in the present study strongly supports findings from human chronic pain patients, whereas the changes in M1/M2 are unique to this study. Motor cortex findings may be due to partial volume effects of the small region size in immediate proximity to the ACC, a region rich in opioid receptors, or may be specific to the SNI model, which involves a partial sectioning of the sciatic nerve. The distribution of the tracer binding observed here in controls is in line with previous findings in rodents and humans suggesting a reasonably high inter-species homology. Specifically, of the brain regions investigated, the highest levels of binding were found in regions known to be densely populated with opioid receptors including the thalamus, PFC, NAc, ACC, PAG, CPu, and amygdala, while the lowest levels were seen in the sensory cortex, visual cortex and cerebellum. Our findings in rat, together with others [33; 42], suggest that these opioid receptor-dense regions in the rat brain correspond to homologous regions in the human brain including the thalamus, anterior cingulate cortex, caudate-putamen and amygdala [5].

4.2. Decreased opioid receptor availability reflects reduced receptor expression

As described in Section 1, there are several potential mechanisms underlying reduced opioid binding. These possibilities can only be discerned by examining the brain tissue where differences were observed with PET. We found reduced mu-opioid receptor immunoreactivity, likely indicating reduced receptor density, without significant reductions in enkephalin content or in the number of neurons.

Anatomical magnetic resonance imaging studies in humans [11] and rodents [49] have demonstrated a consistent pattern of grey matter decreases with chronic pain. However, our current findings, based on immunohistochemical labeling of neuronal markers, do not support the notion of pain-related neurodegeneration in the regions of interest. Indeed, while

one possible explanation for the gray matter decreases is neuronal loss, a recent study suggests that the more likely explanation involves changes in brain water content and neuronal integrity, rather than clear neuronal loss [45], suggesting that the apparent discrepancy may be related to technical differences.

While there is no direct evidence of increased levels of endogenous enkephalin in human chronic pain patients, some have argued that higher levels of endogenously released enkephalin underlie decreased receptor availability in chronic pain states [25; 26]. Studies of supraspinal enkephalin concentrations in rodent models of chronic pain focus mainly on brainstem nuclei including the periaqueductal gray and the rostroventral medulla, where enkephalin levels seem to be transiently increased for no more than 3 weeks after CFA-induced persistent inflammation [24; 35; 39; 54]. In higher brain regions such as the hypothalamus, transient increases in enkephalin also return to basal levels by approximately 3 weeks [39]. In the present study, no differences in enkephalin were observed in either the caudate-putamen or the insula 3 months after nerve injury, suggesting that while relatively short-term changes in endogenous enkephalin levels may occur in rodent models of chronic pain, these increases likely subside despite ongoing hypersensitivity. In the context of our findings, pain-related reduced receptor availability is unlikely to be related to increased enkephalin levels.

Down-regulation of mu-opioid receptors in the rodent spinal cord and dorsal root ganglion can occur within days or a few weeks nerve injury [44; 46; 47; 58]. Our study extends these findings to the brain, suggesting that downregulation of mu-opioid receptors occurs throughout the central nervous system after nerve injury. While we observed significant changes in the mu-opioid receptor system using immunohistochemistry in two of the three regions, it is important to note that [¹⁸F]FDPN binds to mu-, delta- and kappa-opioid receptors with equal affinity. Accordingly, it is possible that delta- and kappa-opioids might also contribute to the lower opioid receptor availability observed with PET. Given that no statistically significant changes in MOR1-ir were found within the posterior insula, investigation of the delta- and kappa-opioid receptor within this region would be a logical extension of this work. However, of the aforementioned human opioid-PET studies investigating chronic pain, no systematic difference exists between those employing [¹⁸F]FDPN and those using a Carfentanil based tracer (which binds specifically to the mu-opioid receptor), suggesting that the mu-opioid receptor system is a significant driver of this effect. As such, it is likely that the changes to the mu-opioid receptor give rise to the observed [¹⁸F]FDPN-PET changes. Taken together, our results strongly support altered expression levels of the mu-opioid receptor as the basis for the observed changes in opioid receptor availability using [¹⁸F]FDPN-PET.

4.3. Anhedonia and chronic pain

Sucrose preference, an assay for anhedonia, was lower in nerve-injured rats compared to controls after three months of nerve injury, in line with previous reports in rodent chronic pain models [2; 9; 52]. Preference for sweet-tasting water progressively increases with age in adult rats [3; 14; 41], an effect that can be prevented by nerve injury [3]. Our findings

match this pattern perfectly, where sucrose preference increased in controls but not in nerve-injured rats.

At three months post-surgery, sucrose preference positively correlated with opioid receptor availability and MOR1-ir in the caudate-putamen of the injured rats. Specifically, while some nerve-injured rats exhibited sucrose preference levels and MOR1 expression that were comparable to sham rats, others showed lower levels of receptor expression along with marked anhedonia. As such, our results seem to correspond with the clinical findings that only a portion of the chronic pain population is depressed [15; 36; 51]. Moreover, while the caudate-putamen is known to play a role in anhedonia/depression [19; 22; 43] and trait anhedonia correlates with anterior caudate volume in humans [22], the striatal opioid system, including the caudate-putamen, can modulate sucrose hedonics and feeding behavior in rats [28; 57]. Therefore, as observed here in rats, the degree of anhedonia/depression observed in human chronic pain patients may also be related to the level of mu-opioid receptor expression in the striatum. Interestingly, while we did observe pain-induced changes to anhedonia that correlated with opioid markers, we did not observe any correlation between hypersensitivity outcomes and opioid markers (post-hoc exploration, data not reported). An intriguing extension to this work would be to attempt to understand the inter-individual differences in anhedonia given that no linear relationship is observed between nociceptive assays and opioid markers.

Stress, especially chronic stress, is considered to be among the best indicators for the development of affective disorders in humans (reviewed in [20; 29]), and comorbid depression has long been posited to be a direct consequence of chronic pain [17; 34]. Here, we provide new evidence that chronic neuropathic pain changes the brain opioid system in rats. Moreover, the degree to which the opioid system is impacted corresponds to the level of anhedonia, a core symptom of major depression in humans [1]. Given the central role that opioid receptors play in pain, reward and addiction, as well as the the time-dependent impact of stress on anhedonia [48], it is not surprising that persistent pain could, over time, affect one's ability to experience pleasure. With the current medical and political controversy regarding the use of opioids in chronic pain patients, improved understanding of the relationship between chronic pain and the endogenous opioid system is crucial to better address issues related to opiate efficacy, addiction and reward.

Supplementary Material

Refer to Web version on PubMed Central for supplementary material.

Acknowledgments

This research was funded by the Intramural Research Programs of the National Center for Complementary and Integrative Health (NCCIH) and the National Institute of Biomedical Imaging and Bioengineering (NIBIB), National Institutes of Health. Orit Jacobson, PhD, National Institutes of Health, assisted with the radiochemistry. Lucy Vulchanova, PhD, Assistant Professor, Department of Neuroscience, University of Minnesota donated the rabbit-derived anti-MOR1. Scott J Thompson was supported by The Louise and Alan Edwards Foundation's Ph.D. Studentship in Pain Research.

References

1. Diagnostic and statistical manual of mental disorders. 5th. Washington DC: American Psychiatric Association; 2013.
2. Amorim D, David-Pereira A, Pertovaara A, Almeida A, Pinto-Ribeiro F. Amitriptyline reverses hyperalgesia and improves associated mood-like disorders in a model of experimental monoarthritis. *Behav Brain Res.* 2014; 265:12–21. [PubMed: 24518202]
3. Andersen ML, Hoshino K, Tufik S. Increased susceptibility to development of anhedonia in rats with chronic peripheral nerve injury: involvement of sleep deprivation? *Prog Neuropsychopharmacol Biol Psychiatry.* 2009; 33(6):960–966. [PubMed: 19414057]
4. Arvidsson U, Riedl M, Chakrabarti S, Lee JH, Nakano AH, Dado RJ, Loh HH, Law PY, Wessendorf MW, Elde R. Distribution and targeting of a mu-opioid receptor (MOR1) in brain and spinal cord. *J Neurosci.* 1995; 15(5 Pt 1):3328–3341. [PubMed: 7751913]
5. Baumgartner U, Buchholz HG, Bellosevich A, Magerl W, Siessmeier T, Rolke R, Hohnemann S, Piel M, Rosch F, Wester HJ, Henriksen G, Stoeter P, Bartenstein P, Treede RD, Schreckenberger M. High opiate receptor binding potential in the human lateral pain system. *Neuroimage.* 2006; 30(3):692–699. [PubMed: 16337817]
6. Bencherif B, Fuchs PN, Sheth R, Dannals RF, Campbell JN, Frost JJ. Pain activation of human supraspinal opioid pathways as demonstrated by [11C]-carfentanil and positron emission tomography (PET). *Pain.* 2002; 99(3):589–598. [PubMed: 12406535]
7. Brown CA, Matthews J, Fairclough M, McMahon A, Barnett E, Al-Kaysi A, El-Dereby W, Jones AK. Striatal opioid receptor availability is related to acute and chronic pain perception in arthritis: does opioid adaptation increase resilience to chronic pain? *Pain.* 2015; 156(11):2267–2275. [PubMed: 26176892]
8. Bruehl S, Apkarian AV, Ballantyne JC, Berger A, Borsook D, Chen WG, Farrar JT, Haythornthwaite JA, Horn SD, Iadarola MJ, Inturrisi CE, Lao L, Mackey S, Mao J, Sawczuk A, Uhl GR, Witter J, Woolf CJ, Zubieta JK, Lin Y. Personalized medicine and opioid analgesic prescribing for chronic pain: opportunities and challenges. *J Pain.* 2013; 14(2):103–113. [PubMed: 23374939]
9. Bura AS, Guegan T, Zamanillo D, Vela JM, Maldonado R. Operant self-administration of a sigma ligand improves nociceptive and emotional manifestations of neuropathic pain. *Eur J Pain.* 2013; 17(6):832–843. [PubMed: 23172791]
10. Bushnell MC, Ceko M, Low LA. Cognitive and emotional control of pain and its disruption in chronic pain. *Nat Rev Neurosci.* 2013; 14(7):502–511. [PubMed: 23719569]
11. Cauda F, Palermo S, Costa T, Torta R, Duca S, Vercelli U, Geminiani G, Torta DM. Gray matter alterations in chronic pain: A network-oriented meta-analytic approach. *Neuroimage Clin.* 2014; 4:676–686. [PubMed: 24936419]
12. Chen L, Vo T, Seefeld L, Malarick C, Houghton M, Ahmed S, Zhang Y, Cohen A, Retamozo C, St Hilaire K, Zhang V, Mao J. Lack of correlation between opioid dose adjustment and pain score change in a group of chronic pain patients. *J Pain.* 2013; 14(4):384–392. [PubMed: 23452826]
13. Choi Y, Yoon YW, Na HS, Kim SH, Chung JM. Behavioral signs of ongoing pain and cold allodynia in a rat model of neuropathic pain. *Pain.* 1994; 59(3):369–376. [PubMed: 7708411]
14. Colavita FB. Saccharine Preference in Rats as a Function of Age and Early Experience. *Psychonomic Science.* 1968; 12(7):311.
15. Currie SR, Wang J. Chronic back pain and major depression in the general Canadian population. *Pain.* 2004; 107(1–2):54–60. [PubMed: 14715389]
16. Decosterd I, Woolf CJ. Spared nerve injury: an animal model of persistent peripheral neuropathic pain. *Pain.* 2000; 87(2):149–158. [PubMed: 10924808]
17. Dohrenwend BP, Raphael KG, Marbach JJ, Gallagher RM. Why is depression comorbid with chronic myofascial face pain? A family study test of alternative hypotheses. *Pain.* 1999; 83(2):183–192. [PubMed: 10534589]
18. Dossantos MF, Martikainen IK, Nascimento TD, Love TM, Deboer MD, Maslowski EC, Monteiro AA, Vincent MB, Zubieta JK, Dasilva AF. Reduced basal ganglia mu-opioid receptor availability in trigeminal neuropathic pain: A pilot study. *Molecular pain.* 2012; 8(1):74. [PubMed: 23006894]

19. Dunn RT, Kimbrell TA, Ketter TA, Frye MA, Willis MW, Luckenbaugh DA, Post RM. Principal components of the Beck Depression Inventory and regional cerebral metabolism in unipolar and bipolar depression. *Biol Psychiatry*. 2002; 51(5):387–399. [PubMed: 11904133]
20. Hammen C. Stress and depression. *Annu Rev Clin Psychol*. 2005; 1:293–319. [PubMed: 17716090]
21. Harris RE, Clauw DJ, Scott DJ, McLean SA, Gracely RH, Zubieta JK. Decreased central mu-opioid receptor availability in fibromyalgia. *The Journal of neuroscience : the official journal of the Society for Neuroscience*. 2007; 27(37):10000–10006. [PubMed: 17855614]
22. Harvey PO, Pruessner J, Czechowska Y, Lepage M. Individual differences in trait anhedonia: a structural and functional magnetic resonance imaging study in non-clinical subjects. *Mol Psychiatry*. 2007; 12(8):703, 767–775. [PubMed: 17505465]
23. Hirvonen J, Aalto S, Hagelberg N, Maksimov A, Ingman K, Oikonen V, Virkkala J, Nagren K, Scheinin H. Measurement of central mu-opioid receptor binding in vivo with PET and [11C]carfentanil: a test-retest study in healthy subjects. *Eur J Nucl Med Mol Imaging*. 2009; 36(2): 275–286. [PubMed: 18779961]
24. Hurley RW, Hammond DL. Contribution of endogenous enkephalins to the enhanced analgesic effects of supraspinal mu opioid receptor agonists after inflammatory injury. *J Neurosci*. 2001; 21(7):2536–2545. [PubMed: 11264327]
25. Jones AK, Cunningham VJ, Ha-Kawa S, Fujiwara T, Luthra SK, Silva S, Derbyshire S, Jones T. Changes in central opioid receptor binding in relation to inflammation and pain in patients with rheumatoid arthritis. *Br J Rheumatol*. 1994; 33(10):909–916. [PubMed: 7921749]
26. Jones AK, Kitchen ND, Watabe H, Cunningham VJ, Jones T, Luthra SK, Thomas DG. Measurement of changes in opioid receptor binding in vivo during trigeminal neuralgic pain using [11C] diprenorphine and positron emission tomography. *Journal of cerebral blood flow and metabolism : official journal of the International Society of Cerebral Blood Flow and Metabolism*. 1999; 19(7):803–808.
27. Jones AK, Watabe H, Cunningham VJ, Jones T. Cerebral decreases in opioid receptor binding in patients with central neuropathic pain measured by [11C]diprenorphine binding and PET. *European journal of pain*. 2004; 8(5):479–485. [PubMed: 15324779]
28. Kelley AE, Bakshi VP, Haber SN, Steininger TL, Will MJ, Zhang M. Opioid modulation of taste hedonics within the ventral striatum. *Physiol Behav*. 2002; 76(3):365–377. [PubMed: 12117573]
29. Kessler RC. The effects of stressful life events on depression. *Annu Rev Psychol*. 1997; 48:191–214. [PubMed: 9046559]
30. Klega A, Eberle T, Buchholz HG, Maus S, Maihofner C, Schreckenberger M, Birklein F. Central opioidergic neurotransmission in complex regional pain syndrome. *Neurology*. 2010; 75(2):129–136. [PubMed: 20625165]
31. Liu YT, Shao YW, Yen CT, Shaw FZ. Acid-induced hyperalgesia and anxio-depressive comorbidity in rats. *Physiol Behav*. 2014; 131:105–110. [PubMed: 24726391]
32. Maarrawi J, Peyron R, Mertens P, Costes N, Magnin M, Sindou M, Laurent B, Garcia-Larrea L. Differential brain opioid receptor availability in central and peripheral neuropathic pain. *Pain*. 2007; 127(1–2):183–194. [PubMed: 17137714]
33. Melichar JK, Hume SP, Williams TM, Daghli MR, Taylor LG, Ahmad R, Malizia AL, Brooks DJ, Myles JS, Lingford-Hughes A, Nutt DJ. Using [11C]diprenorphine to image opioid receptor occupancy by methadone in opioid addiction: clinical and preclinical studies. *J Pharmacol Exp Ther*. 2005; 312(1):309–315. [PubMed: 15347732]
34. Merikangas KR, Risch NJ, Merikangas JR, Weissman MM, Kidd KK. Migraine and depression: association and familial transmission. *J Psychiatr Res*. 1988; 22(2):119–129. [PubMed: 3404480]
35. Millan MJ, Morris BJ, Colpaert FC, Herz A. A model of chronic pain in the rat: high-resolution neuroanatomical approach identifies alterations in multiple opioid systems in the periaqueductal grey. *Brain Res*. 1987; 416(2):349–353. [PubMed: 3040180]
36. Miller LR, Cano A. Comorbid chronic pain and depression: who is at risk? *J Pain*. 2009; 10(6): 619–627. [PubMed: 19398383]
37. Navratilova E, Porreca F. Reward and motivation in pain and pain relief. *Nat Neurosci*. 2014; 17(10):1304–1312. [PubMed: 25254980]

38. Noble M, Treadwell JR, Tregear SJ, Coates VH, Wiffen PJ, Akafomo C, Schoelles KM. Long-term opioid management for chronic noncancer pain. *Cochrane Database Syst Rev.* 2010; 1:CD006605.
39. Panerai AE, Sacerdote P, Bianchi M, Brini A, Mantegazza P. Brain and spinal cord neuropeptides in adjuvant induced arthritis in rats. *Life Sci.* 1987; 41(10):1297–1303. [PubMed: 2442576]
40. Paxinos G, Watson C. *The rat brain in stereotaxic coordinates.* Amsterdam; Boston: Academic Press/Elsevier; 2007.
41. Perez C, Sclafani A. Developmental changes in sugar and starch taste preferences in young rats. *Physiol Behav.* 1990; 48(1):7–12. [PubMed: 2236280]
42. Pert CB, Snyder SH. Opiate receptor: demonstration in nervous tissue. *Science.* 1973; 179(4077):1011–1014. [PubMed: 4687585]
43. Pizzagalli DA, Holmes AJ, Dillon DG, Goetz EL, Birk JL, Bogdan R, Dougherty DD, Iosifescu DV, Rauch SL, Fava M. Reduced caudate and nucleus accumbens response to rewards in unmedicated individuals with major depressive disorder. *Am J Psychiatry.* 2009; 166(6):702–710. [PubMed: 19411368]
44. Pol O, Murtra P, Caracuel L, Valverde O, Puig MM, Maldonado R. Expression of opioid receptors and c-fos in CB1 knockout mice exposed to neuropathic pain. *Neuropharmacology.* 2006; 50(1):123–132. [PubMed: 16360182]
45. Pomares FB, Funck T, Feier NA, Roy S, Daigle-Martel A, Ceko M, Narayanan S, Araujo D, Thiel A, Stikov N, Fitzcharles MA, Schweinhardt P. Histological Underpinnings of Grey Matter Changes in Fibromyalgia Investigated Using Multimodal Brain Imaging. *J Neurosci.* 2017; 37(5):1090–1101. [PubMed: 27986927]
46. Porreca F, Tang QB, Bian D, Riedl M, Elde R, Lai J. Spinal opioid mu receptor expression in lumbar spinal cord of rats following nerve injury. *Brain Res.* 1998; 795(1–2):197–203. [PubMed: 9622629]
47. Rashid MH, Inoue M, Toda K, Ueda H. Loss of peripheral morphine analgesia contributes to the reduced effectiveness of systemic morphine in neuropathic pain. *J Pharmacol Exp Ther.* 2004; 309(1):380–387. [PubMed: 14718584]
48. Rygula R, Abumaria N, Flugge G, Fuchs E, Ruther E, Havemann-Reinecke U. Anhedonia and motivational deficits in rats: impact of chronic social stress. *Behav Brain Res.* 2005; 162(1):127–134. [PubMed: 15922073]
49. Seminowicz DA, Laferriere AL, Millicamps M, Yu JS, Coderre TJ, Bushnell MC. MRI structural brain changes associated with sensory and emotional function in a rat model of long-term neuropathic pain. *NeuroImage.* 2009; 47(3):1007–1014. [PubMed: 19497372]
50. Sprenger T, Willoch F, Miederer M, Schindler F, Valet M, Berthele A, Spilker ME, Forderreuther S, Straube A, Stangier I, Wester HJ, Tolle TR. Opioidergic changes in the pineal gland and hypothalamus in cluster headache: a ligand PET study. *Neurology.* 2006; 66(7):1108–1110. [PubMed: 16606930]
51. Tsang A, Von Korff M, Lee S, Alonso J, Karam E, Angermeyer MC, Borges GL, Bromet EJ, Demyttenaere K, de Girolamo G, de Graaf R, Gureje O, Lepine JP, Haro JM, Levinson D, Oakley Browne MA, Posada-Villa J, Seedat S, Watanabe M. Common chronic pain conditions in developed and developing countries: gender and age differences and comorbidity with depression-anxiety disorders. *J Pain.* 2008; 9(10):883–891. [PubMed: 18602869]
52. Wang J, Goffer Y, Xu D, Tukey DS, Shamir DB, Eberle SE, Zou AH, Blanck TJ, Ziff EB. A single subanesthetic dose of ketamine relieves depression-like behaviors induced by neuropathic pain in rats. *Anesthesiology.* 2011; 115(4):812–821. [PubMed: 21934410]
53. Wester HJ, Willoch F, Tolle TR, Munz F, Herz M, Oye I, Schadrack J, Schwaiger M, Bartenstein P. 6-O-(2-[18F]fluoroethyl)-6-O-desmethyldiprenorphine ([18F]DPN): synthesis, biologic evaluation, and comparison with [11C]DPN in humans. *J Nucl Med.* 2000; 41(7):1279–1286. [PubMed: 10914922]
54. Williams FG, Mullet MA, Beitz AJ. Basal release of Met-enkephalin and neurotensin in the ventrolateral periaqueductal gray matter of the rat: a microdialysis study of antinociceptive circuits. *Brain Res.* 1995; 690(2):207–216. [PubMed: 8535838]

55. Willoch F, Schindler F, Wester HJ, Empl M, Straube A, Schwaiger M, Conrad B, Tolle TR. Central poststroke pain and reduced opioid receptor binding within pain processing circuitries: a [¹¹C]diprenorphine PET study. *Pain*. 2004; 108(3):213–220. [PubMed: 15030940]
56. Zhang GF, Wang J, Han JF, Guo J, Xie ZM, Pan W, Yang JJ, Sun KJ. Acute single dose of ketamine relieves mechanical allodynia and consequent depression-like behaviors in a rat model. *Neurosci Lett*. 2016; 631:7–12. [PubMed: 27497920]
57. Zhang M, Kelley AE. Enhanced intake of high-fat food following striatal mu-opioid stimulation: microinjection mapping and fos expression. *Neuroscience*. 2000; 99(2):267–277. [PubMed: 10938432]
58. Zhang X, Bao L, Shi TJ, Ju G, Elde R, Hokfelt T. Down-regulation of mu-opioid receptors in rat and monkey dorsal root ganglion neurons and spinal cord after peripheral axotomy. *Neuroscience*. 1998; 82(1):223–240. [PubMed: 9483516]
59. Zhang X, de Araujo Lucas G, Elde R, Wiesenfeld-Hallin Z, Hokfelt T. Effect of morphine on cholecystokinin and mu-opioid receptor-like immunoreactivities in rat spinal dorsal horn neurons after peripheral axotomy and inflammation. *Neuroscience*. 2000; 95(1):197–207. [PubMed: 10619476]
60. Zubieta JK, Bueller JA, Jackson LR, Scott DJ, Xu Y, Koeppe RA, Nichols TE, Stohler CS. Placebo effects mediated by endogenous opioid activity on mu-opioid receptors. *The Journal of neuroscience : the official journal of the Society for Neuroscience*. 2005; 25(34):7754–7762. [PubMed: 16120776]
61. Zubieta JK, Smith YR, Bueller JA, Xu Y, Kilbourn MR, Jewett DM, Meyer CR, Koeppe RA, Stohler CS. Regional mu opioid receptor regulation of sensory and affective dimensions of pain. *Science*. 2001; 293(5528):311–315. [PubMed: 11452128]
62. Zubieta JK, Smith YR, Bueller JA, Xu Y, Kilbourn MR, Jewett DM, Meyer CR, Koeppe RA, Stohler CS. Mu-opioid receptor-mediated antinociceptive responses differ in men and women. *The Journal of neuroscience : the official journal of the Society for Neuroscience*. 2002; 22(12):5100–5107. [PubMed: 12077205]

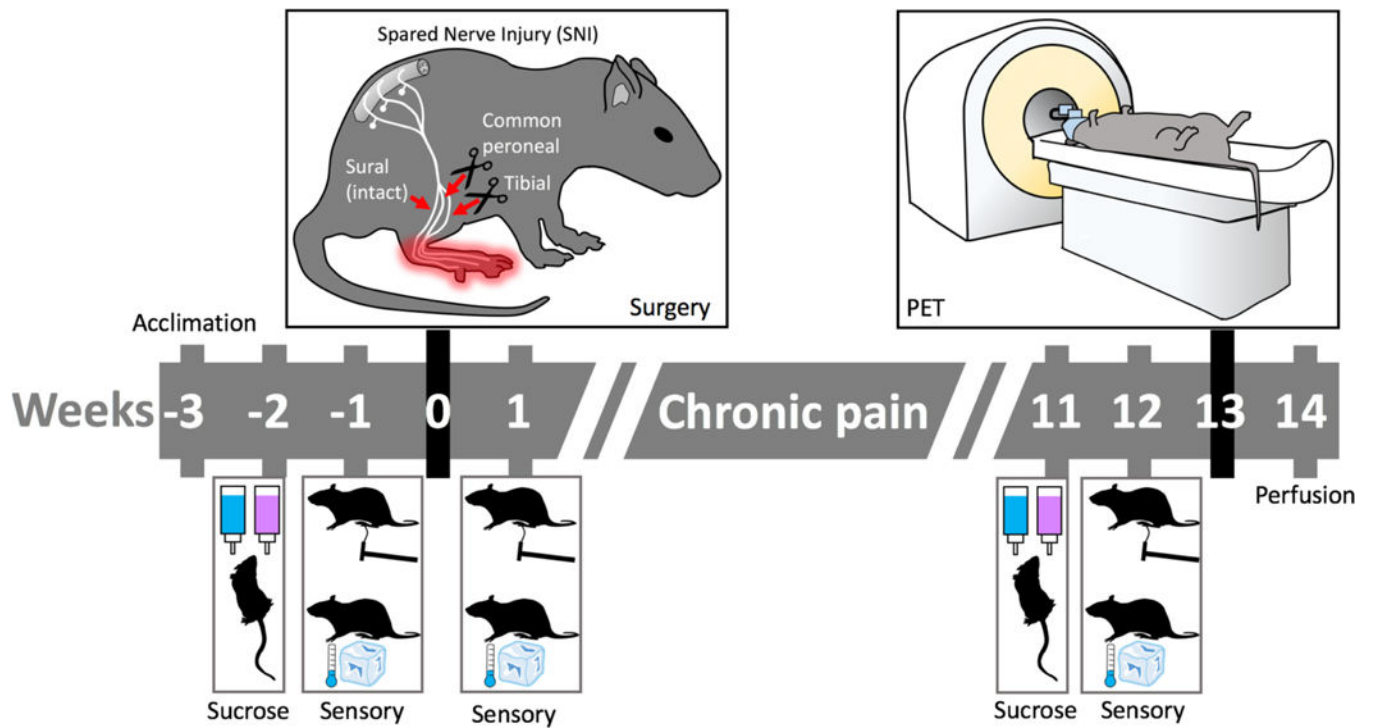


Fig. 1. Study design

Behavioral testing for mechanical and cold sensitivity was performed prior to surgery and again one week and three months after surgery. Rats were tested for sucrose preference as an index of anhedonia before surgery and again three months after surgery. [^{18}F]FDPN-PET was performed at week 13 followed by tissue fixation for immunohistochemistry at week 14.

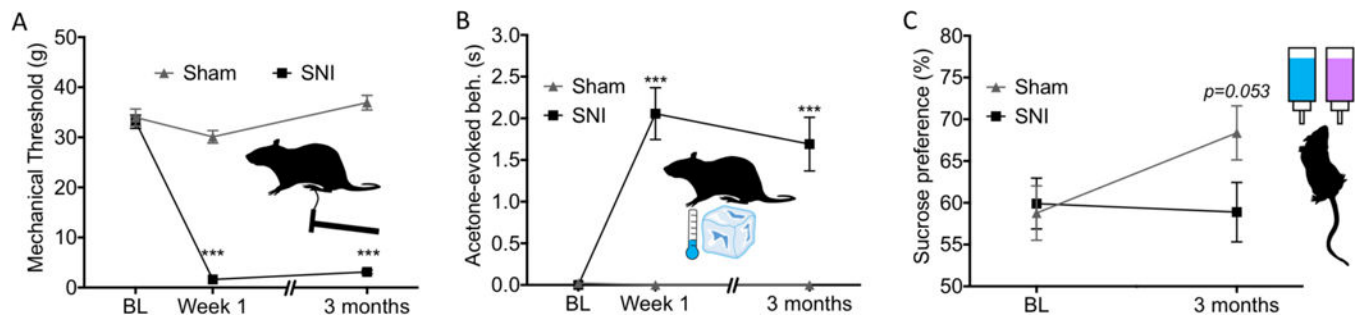


Fig. 2. Neuropathic pain-induced deficits in hypersensitivity and anhedonia

(A) Repeated measures two-way ANOVA analysis of mechanical thresholds yielded a significant group \times time effect ($F_{2,86} = 94.7$, $p < 0.001$). While posthoc assessment showed no difference in mechanical threshold between the two groups pre-surgery, at both one week and three months post-surgery, nerve-injured rats had a significantly lower withdrawal thresholds compared to controls. (B) A significant group \times time effect ($F_{2,86} = 17.5$, $p < 0.001$) was also found for cold sensitivity. Post-hoc analysis showed significant differences between groups at both post-surgery time points but not at baseline. (C) Repeated measures two-way ANOVA analysis of sucrose preference yielded a significant group \times time effect ($F_{1,43} = 5.02$, $p = 0.030$). Data are presented as mean \pm S.E.M. *** = $p < 0.001$ compared to control group. BL = Baseline.

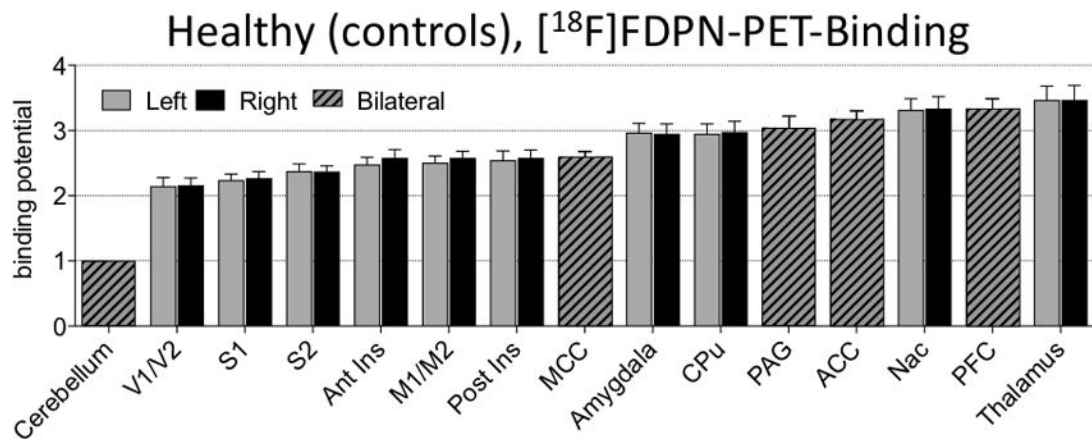


Fig. 3. [¹⁸F]-FDPN tracer binding in control rat brain to validate the tracer

Values displayed are normalized with the cerebellum as reference region, mean +/- standard deviation. A one-way ANOVA contrasting all brain regions was found to be significant $F_{22,368} = 284.251$, $p < 0.001$ with posthoc analysis contrasting each brain region to the cerebellum found each region to be significantly different than the cerebellum which is devoid of opioid receptors ($p < 0.001$).

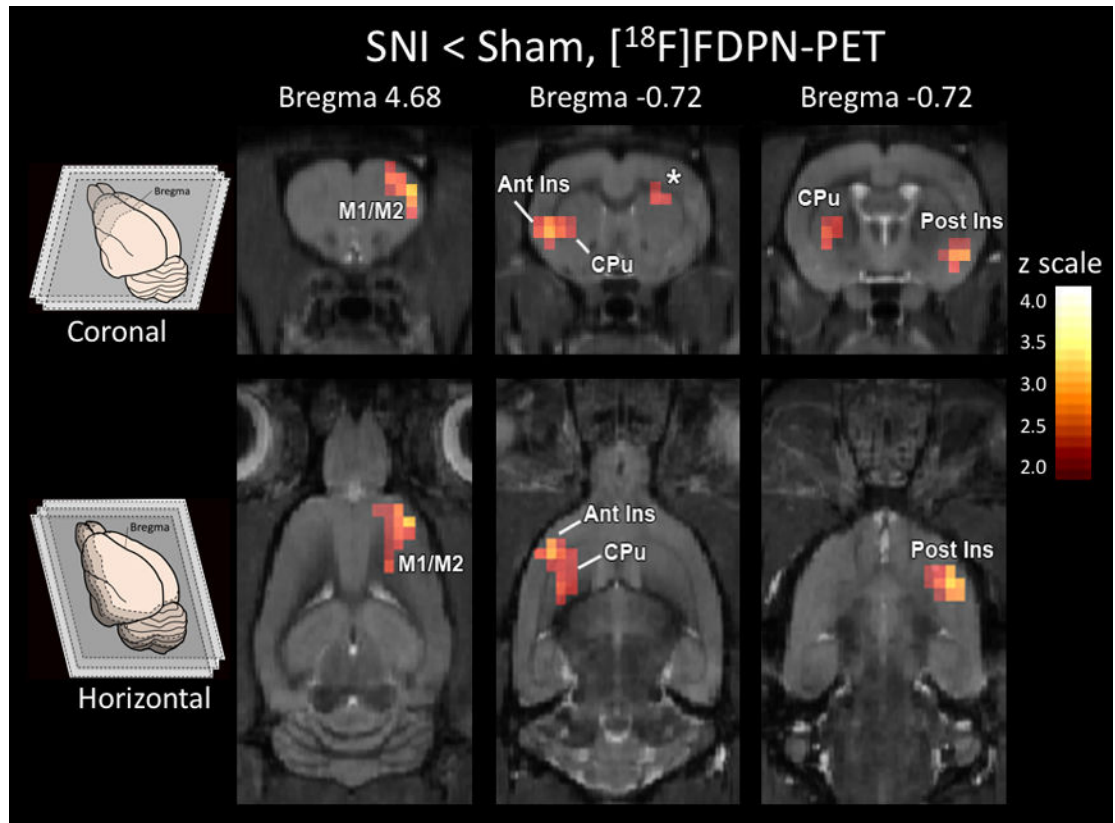


Fig. 4. Reduced opioid receptor availability in the striatum

Less opioid receptor availability ($p < 0.01$, cluster corrected) was observed in nerve-injured rats than control rats in ipsilateral anterior insula (Ant Ins), ipsilateral caudate-putamen (CPu), contralateral posterior insula (Post Ins) and contralateral M1/M2. There were no clusters nor any single voxels that exceeded the significance threshold for the contrast of SNI > sham.

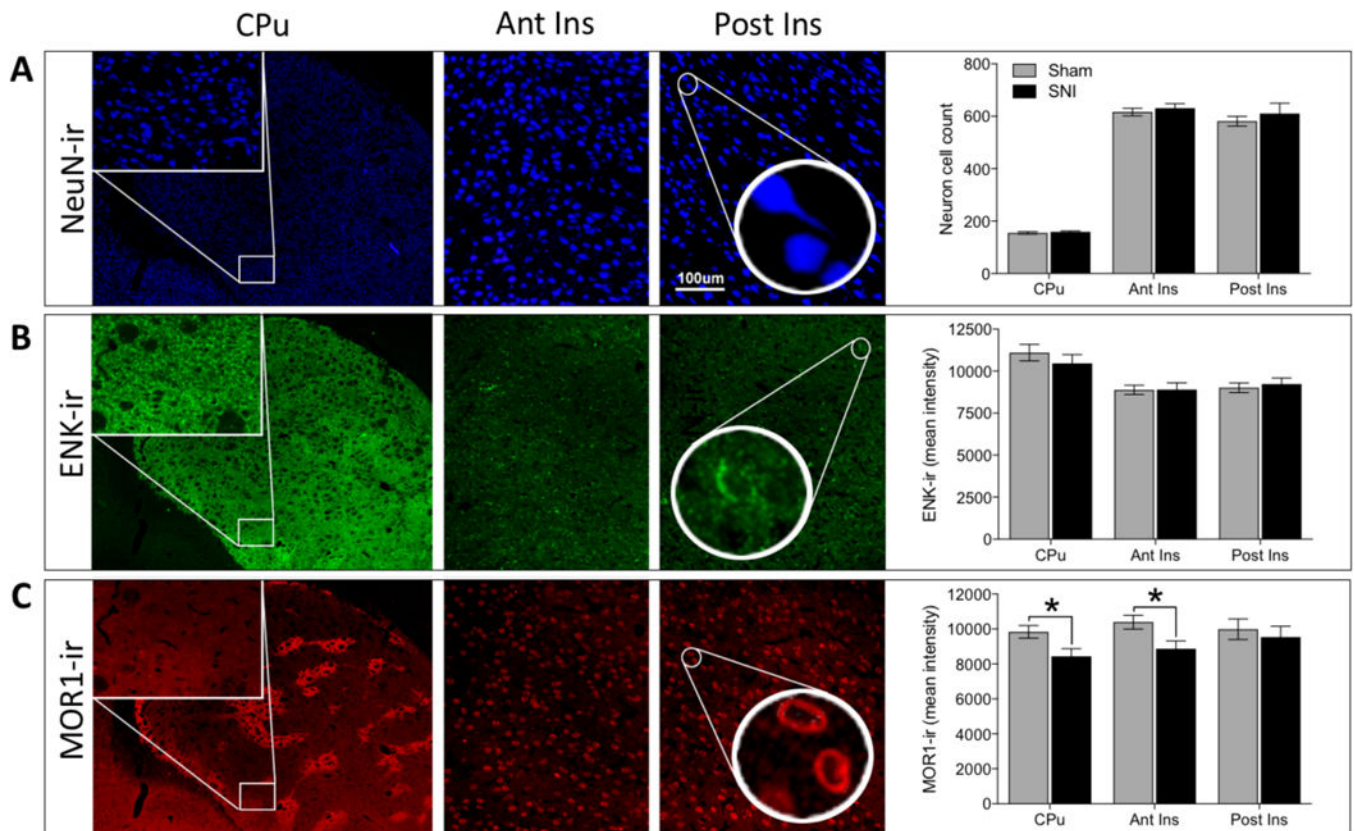


Fig. 5. Reduced MOR1 expression in the striatum

(A) Representative images and quantification of NeuN-ir, neuron cell body count.

Representative images taken from caudate-putamen (CPu) at 4× magnification (insets at 20× represent region of CPu used for analysis), as well as anterior insula (Ant Ins) and posterior insula (Post Ins) at 20× magnification. No significant difference in neuronal cell body count was observed between nerve-injured and control rats ($F_{1,42} = 0.936$, $p = 0.339$).

(B) Representative images and quantification of ENK-ir (enkephalin immunoreactivity). No significant difference in ENK-ir was observed between nerve-injured and control rats ($F_{1,42} = 0.166$, $p = 0.685$).

(C) Representative images and quantification of MOR1-ir (mu-opioid receptor immunoreactivity). A significant difference in MOR1-ir was observed between groups over three brain regions ($F_{1,42} = 8.092$, $p = 0.007$). Posthoc tests showed chronic pain to be associated with lower MOR1-ir intensity in two of the three brain regions: CPu (SNI = 8437 ± 437 ; Sham = 9832 ± 358 ; $p = 0.048$) and anterior insula (SNI = 8862 ± 452 ; Sham = 10390 ± 398 ; $p = 0.031$). Posterior insula (SNI = 9531 ± 620 ; Sham = 9986 ± 587 ; $p = 0.510$) was not significantly different between groups. * = $p < 0.05$.

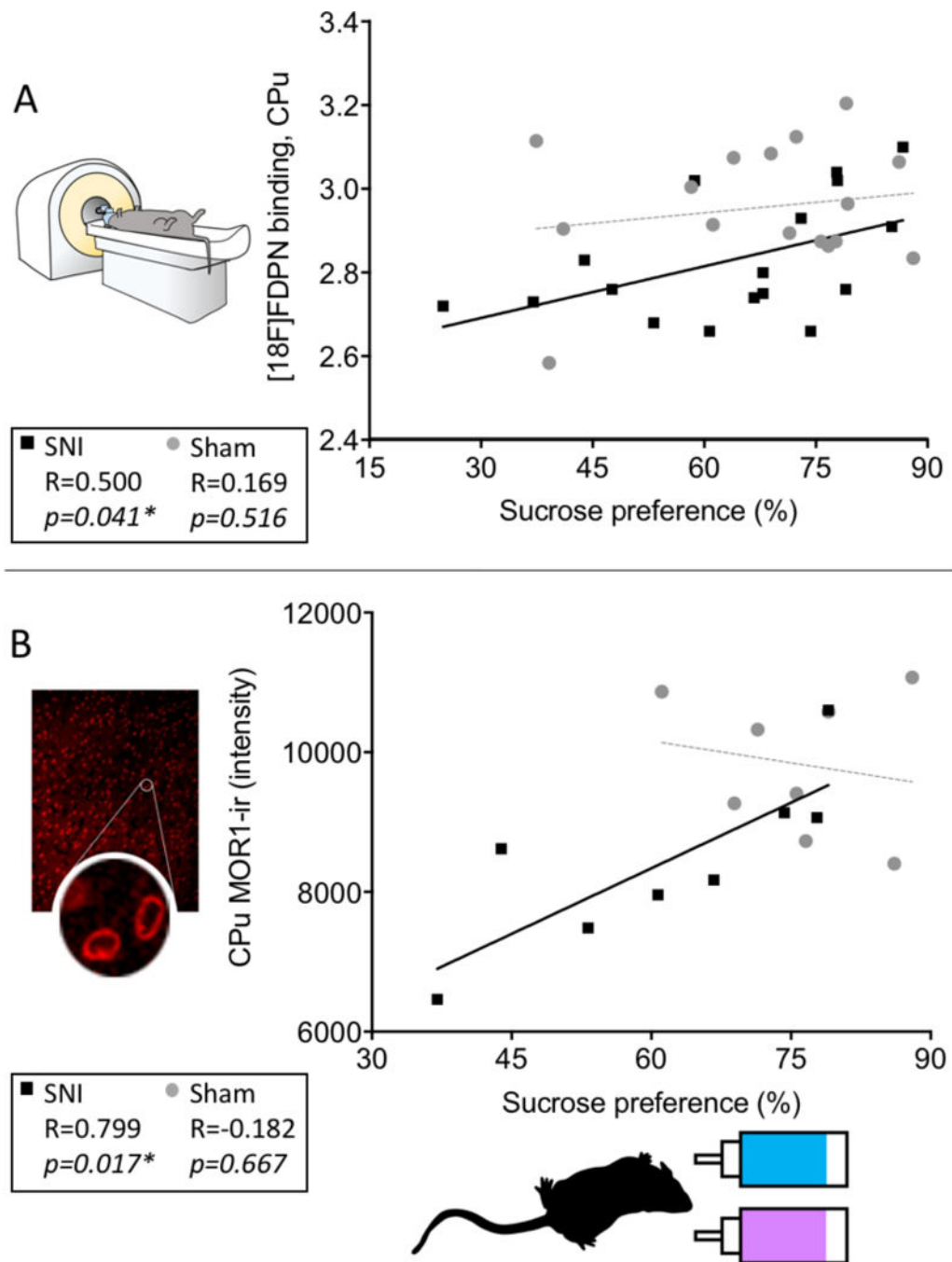


Fig. 6. Post-injury sucrose hedonics positively associated with [¹⁸F]-FDPN binding and MOR1 expression in the Cpu

(A) Sucrose preference scores of the nerve-injured rats at three months post-surgery were positively correlated with opioid receptor availability in the caudate-putamen ($R = 0.500$, $p = 0.041$, $n = 17$) as well as with (B) MOR1-ir intensity in the caudate-putamen ($R = 0.799$, $p = 0.017$, $n = 8$). Sucrose preference for the sham group was not significantly correlated with either (A) opioid receptor availability ($R = 0.169$, $p = 0.516$) or (B) MOR1-ir intensity ($R = 0.182$, $p = 0.667$). $P < 0.05$ was considered significant in all cases. * = $p < 0.05$.